Volume 6
Number 12
21 June 2025
Pages 3745–4146

Materials Advances

rsc.li/materials-advances

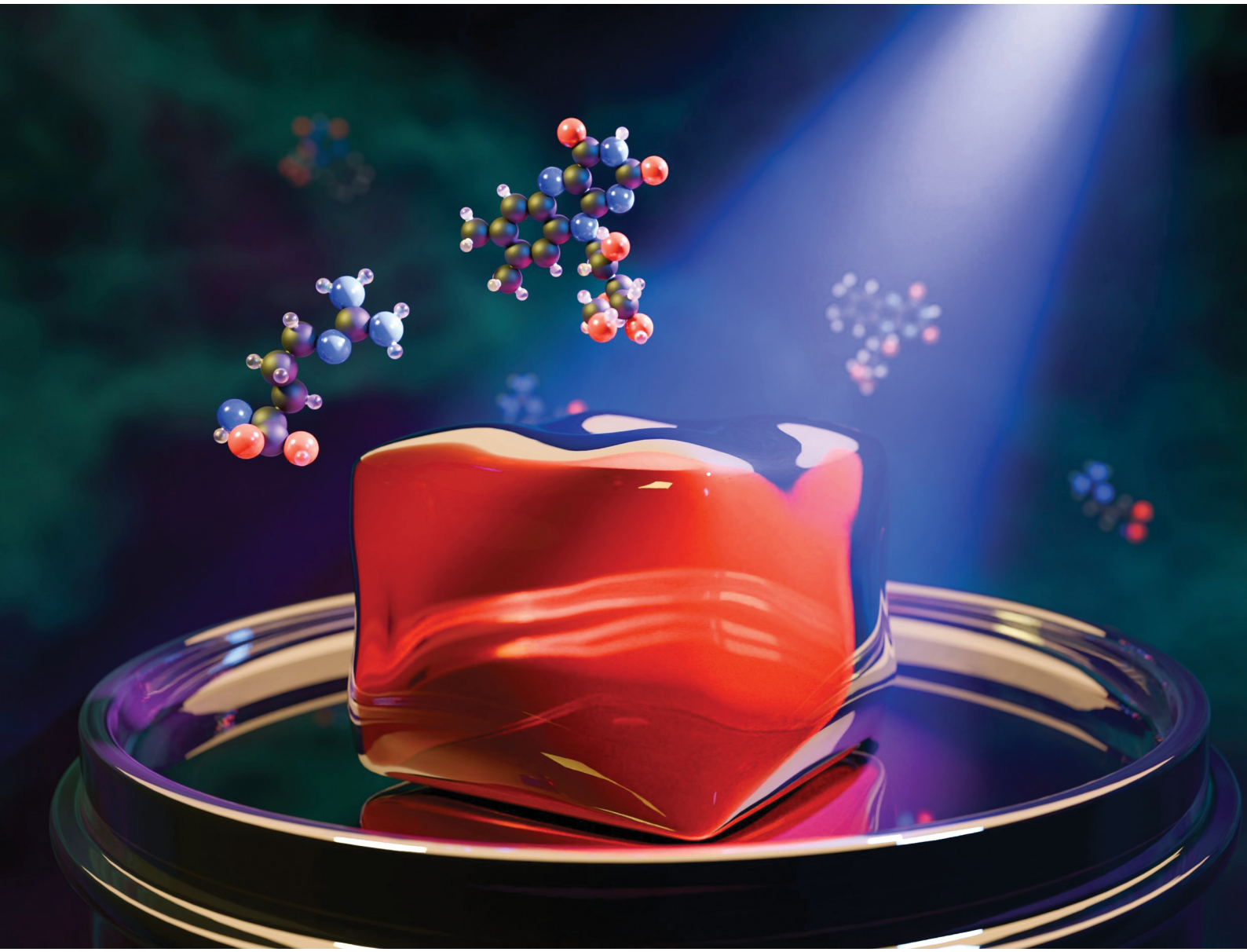

ISSN 2633-5409

ROYAL SOCIETY OF CHEMISTRY

PAPER

Daniela Duarte Campos *et al.*
Biobased photocrosslinkable gelatin-methacrylate hydrogels promote the growth and phenotype maintenance of human corneal keratocytes

Materials Advances

ROYAL SOCIETY OF CHEMISTRY

PAPER

View Article Online
View Journal | View Issue

Cite this: *Mater. Adv.*, 2025, 6, 3805

Biobased photocrosslinkable gelatin-methacrylate hydrogels promote the growth and phenotype maintenance of human corneal keratocytes†

Friederike Dehli,[a] Olivia Schless,[a] Meret Kaliske,[a] Isabel Potthof,[a] Alexandre Taoum,[a] Matthias Fuest[b] and Daniela Duarte Campos *[a]

Received 30th January 2025,
Accepted 20th April 2025

DOI: 10.1039/d5ma00076a

rsc.li/materials-advances

Light-initiated crosslinking of hydrogels is a promising approach for the controlled fabrication of 3D environments in tissue engineering. One of the most fundamental challenges to overcome in light-based hydrogel systems is to maintain high cell viability and phenotype conservation while also minimizing the negative impact of photoinitiation systems on the environment. In this study, a novel photocrosslinkable hydrogel system based on gelatin methacryloyl, and using riboflavin and arginine as natural photoinitiator and co-initiator, respectively, (RA-GelMA) is reported. Photocrosslinking of RA-GelMA is induced by visible light, and the gelation point can be adjusted between 42 and 300 s by changing the concentration of co-initiator or polymer. Depending on the co-initiator concentration, irradiation time, and irradiation intensity, gels with a storage modulus between 2.5 and 17 kPa are produced. Sustained *in vitro* culture of both immortalized and primary human corneal keratocytes as well as cell spreading and phenotype maintenance of primary human corneal keratocytes can be achieved by optimizing the arginine concentration and the irradiation time. This study contributes to the development of sustainable and cell-friendly hydrogel systems as alternatives to state-of-the-art light-triggered hydrogel systems, which are based on synthetic photoinitiators such as LAP or Irgacure, promising for corneal tissue engineering.

1. Introduction

Gelatin methacryloyl (GelMA) hydrogels are often regarded as the "gold standard" in biomaterials science, given their biocompatibility, biodegradability, and ease of modification.[1–3] They are widely used in multiple research fields, including drug delivery,[4,5] bioprinting,[6,7] and tissue engineering.[8,9] Especially in the field of tissue engineering, the use of GelMA has gained traction over the past years, due to its easy processability compared to ECM-derived polymers such as collagen or hyaluronic acid, and to its tunable properties[7] that allow for a wide range of hard and soft tissue engineering applications.[10] Within the field of soft tissue engineering, corneal tissue engineering aims at the regeneration or restoration of corneal injuries or defects and has high translational potential into clinical practice. Blindness caused by corneal injuries or defects affect over one million patients every year,[11] however, treatment options are often limited due to the low availability of healthy donor corneas.[12] Thus, the generation of an artificial cornea is of great interest. The most commonly used approach towards generating an artificial cornea is the fabrication of cell-laden hydrogel constructs[13,14] that can either be transplanted into the eye[13] or even printed *in situ*. Hydrogels used for this purpose are often based on collagen or, more recently, GelMA.[15,16] Collagen is the most widely used matrix, as it is the main constituent in the corneal stroma, however, it is only soluble at low pH, which complicates cell encapsulation, and hydrogels have a lower stiffness ($G' < 5$ kPa) compared to the human cornea (E = 7.5–110 kPa).[17] By contrast, GelMA has higher stiffness (G' = 3–100 kPa),[3,7] which is more similar to the human cornea, and it is soluble at neutral pH. GelMA is a semisynthetic polymer produced by methacryloylation of amine and hydroxy groups in gelatin,[18] which allows for radical crosslinking of polymer chains. During the modification, many beneficial properties of gelatin, such as motifs for biodegradation, are preserved. Recently, GelMA-based hydrogels have also been used in *e.g.* bone,[19] adipose,[20] or cartilage tissue engineering.[21]

[a] *Zentrum für Molekulare Biologie, Universität Heidelberg, Im Neuenheimer Feld 329, 69120 Heidelberg, Germany. E-mail: f.dehli@zmbh.uni-heidelberg.de, olivia.schless@stud.uni-heidelberg.de, meret.kaliske@stud.uni-heidelberg.de, Potthof@stud.uni-heidelberg.de, a.taoum@zmbh.uni-heidelberg.de, d.campos@uni-heidelberg.de*

[b] *Department of Ophthalmology, RWTH Aachen University, Pauwelsstrasse 30, 52074, Aachen, Germany. E-mail: mfuest@ukaachen.de*

† Electronic supplementary information (ESI) available. See DOI: https://doi.org/10.1039/d5ma00076a

GelMA-hydrogels are usually produced by light induced crosslinking of polymer chains, as this technique offers excellent spatiotemporal control over hydrogel formation.[22] The standard photoinitiatiors are either LAP[1,23] or Irgacure 2959,[24] which initiate crosslinking by dissociation into radicals upon irradiation with UV-A light (LAP, Irgacure, 365 nm)[22] or violet light (LAP, 405 nm).[25] While these photoinitiators are generally considered non-cytotoxic at low concentrations,[22] and are typically linked to high cell viability, they have to be synthesized from non-natural, fossil-based compounds. Due to the potential negative impacts associated with the use of these compounds, such as high energy consumption during manufacturing, or limited biodegradation, current biomaterials research aims at shifting toward biobased photoinitiators.

To date, many natural compounds, such as coumarin, anthraquinones, chalcones or flavones have been examined for the polymerization of hydrophobic acrylates or methacrylates.[26–29] However, their relatively low water solubility and their low efficiency often limits their effectiveness when synthesizing hydrogels. One exception is riboflavin (vitamin B_2), a non-toxic compound that has previously been used in UV-A initiated crosslinking of collagen for hydrogel formation[17] or keratoconus treatment.[30] While this demonstrates that riboflavin is a promising candidate for substituting synthetic photoinitiators with natural compounds in hydrogel synthesis, one drawback is that the mechanical properties can only be tuned in a narrow range, and scaffolds typically have a low stiffness (<5 kPa).[17] Riboflavin and riboflavin derivatives have also been used as photoinitiators for the preparation of bioinert poly(ethyleneglycol)diacrylate hydrogels (two-photon-polymerization, 780 nm)[31] or for blue-light (455 nm) induced controlled radical polymerization of methyl methacrylate.[32]

Compared to commonly used photoinitiators, the photoinitiation mechanism in riboflavin-based systems is very complex.[33,34] Radical formation is proposed to be induced by excitation of riboflavin to a biradical triplet state, which usually reacts with a suitable donor molecule, or molecular oxygen.[17] In some cases, acceptor molecules are also used.[33] A suitable donor molecule can be the ribityl tail,[33] or a co-initiator molecule present in the solution.[35] Commonly used co-initiators are organic compounds such as triethylamine[36] or triethanolamine,[31] which can act as hydrogen donors to create radicals. While these molecules improve the crosslinking process considerably, they are often associated with increased cytotoxicity.[37] In this study, we use a novel hydrogel formulation based on riboflavin, GelMA, and arginine (RA-GelMA), which was crosslinked using blue visible light (455 nm). By using the amino acid arginine as co-initiator, which might act as a hydrogen donor due to its amine groups, the photoinitiation system becomes completely biobased. This is an important step in developing more sustainable hydrogel formulations for safer corneal tissue regeneration, especially toward its future use in patients. The crosslinking behavior of RA-GelMA is studied *via* photorheology to optimize the co-initiator and polymer concentration. Furthermore, the influence of different crosslinking parameters on the gel properties is determined, and the biocompatibility of the RA-GelMA formulation is assessed by cytotoxicity tests. Based on the obtained results, we investigate the potential use of RA-GelMA for corneal keratocyte encapsulation, including analysis of viability, spreading, and phenotype maintenance.

2. Experimental

2.1 Chemicals

All chemicals were used without further purification. Gelatin type B (bovine skin, 225 bloom), methacrylic anhydride, arginine hydrochloride, riboflavin, MTT cell proliferation kit and sodium dodecyl sulfate were purchased from Sigma Aldrich. Trimethylsilylpropionate, D_2O bovine serum albumin (BSA) and Trypan Blue (0.4%) were purchased from Carl Roth. DPBS, trypsin/EDTA (0.25% Trypsin, 0.02% EDTA) solution, and Invitrogen™ LIVE/DEAD™ Viability/Cytotoxicity Kit (Calcein AM: 4 mM, Ethidium Homodimer: 2 mM) were purchased from fisher scientific. Paraformaldehyde (8%w/v) and Triton X-100 were purchased from VWR. Alexa Fluor 488 phalloidin (300U) and Alexa Fluor 594 phalloidin (300U) were purchased from Thermo Fisher. Hoechst was purchased from abcam. Antibodies against ALDH1A1 (monocl., IgG mouse, 1–1.5 mg mL^{-1}, 60171-1-Ig) and ALDH3A1 (monocl., IgG1 mouse, 1 mg mL^{-1}, 68036-1-Ig) were purchased from proteintech. Antibodies against keratocan (polycl., IgG rabbit, 1 μg mL^{-1}, bs-11054R) and lumican (polycl., IgG rabbit, 1 μg mL^{-1}, bs-5890R) were purchased from Thermo Fisher (Bioss). Antibodies against alpha-SMA (monocl., IgG2a, mouse, 40 μg mL^{-1}, MA5-11547) were purchased from Thermo Fisher (Invitrogen). Secondary antibodies were purchased from abcam (goat against mouse – Alexa 488, 2 mg mL^{-1}, ab150113, and donkey against rabbit – Alexa 647, 2 mg mL^{-1}, ab150075). Goat serum and donkey serum were purchased from panbiotech.

2.2 Synthesis of GelMA

GelMA was synthesized according to a procedure described by Claaßen *et al.*[38] Briefly, 25.75 g of gelatin type B was dissolved in 250 ml deionized water at a temperature of 40 °C. The temperature was lowered to 37 °C and 13 mL of methacrylic anhydride was added. The pH was adjusted to 7.3 by continuous addition of 4 M NaOH *via* an automatic titrator (T50, Mettler Toledo, Germany). The reaction time was 5 h. Afterward, the reaction mixture was filtered and the crude product was stored at 8 °C for two days. The synthesized GelMA was purified by dialysis against deionized water using a 12–14 kDa MW cutoff dialysis membrane (Sigma Aldrich). The dialysis was done for 5 days, changing the water twice a day. ^{1}H-NMR (300 MHz) in D_2O was used to determine the degree (DM) of methacryloylation using TMSP as an internal standard. The DM was 0.72 mmol g^{-1} or 0.82 mmol g^{-1}. GelMA with a DM of 0.77 mmol g^{-1} was used for all experimental work, except for the encapsulation of HCKi (610 mmol arginine hydrochloride, 2 min irradiation time, see Section 2.8), where GelMA with a DM of 0.85 mmol g^{-1} was used.

2.3 Oscillatory rheology

Photorheology was conducted using a Discovery Hybrid 20 rheometer (TA Instruments, US), equipped with a 12 mm parallel plate geometry and a light curing accessory (TA Instruments, US, consisting of a quartz glass plate and a light source mount). A LED (455 nm emission maximum mounted LED, Thorlabs) was connected to the light curing accessory *via* a 5 mm liquid light guide (Thorlabs, Germany). The irradiation intensity was set to 4.3 mW cm^{-2}, and it was measured using a Si photodiode power meter (Thorlabs, Germany). A fixed measuring gap of 270 μm was used and the samples were sheared with a frequency of 1 Hz and a strain of 1%. The light source was switched on after 20 s. This time period was subtracted from the obtained values for the gelation point (t_g) to obtain the results displayed in Section 3.1. The gelation point was defined as the intersection of storage modulus and loss modulus (G'') and marks the time needed for network formation.[39] All solutions contained 190 μmol L^{-1} (solubility limit) riboflavin and were prepared in PBS.

2.4 Rotational rheology

The viscosity of a 30 wt% GelMA solution in PBS containing 190 mmol mL^{-1} and 610 mmol mL^{-1} arginine hydrochloride at 25 °C was measured using a Discovery Hybrid 20 rheometer (TA Instruments, US) equipped with a 20 mm cone with an angle of 0.5°. The measuring gap was 310 μm and shear rates were between 2–600 s^{-1}.

2.5 Gel characterization

Hydrogel preparation. Hydrogels for material characterization were cast into PDMS molds with a diameter of 8 mm and a height of 2 mm. 30 wt% GelMA solutions were prepared in PBS with 190 μmol L^{-1} riboflavin and varying arginine hydrochloride concentrations. The samples were irradiated with a blue light LED (Thorlabs, Germany, 455 nm emission maximum) with different irradiation intensities and different irradiation times.

Oscillatory rheology. Samples were swollen to equilibrium in PBS buffer for at least 48 h. Afterward, measurements were carried out with a Discovery Hybrid 20 rheometer (TA Instruments, US) equipped with an 8 mm parallel plate geometry. Before each measurement, the diameter of the hydrogels was adjusted to 8 mm using a punch and residual water was removed from the hydrogels by blotting. An amplitude sweep (f = 1 Hz, 0.01% ≤ γ ≤ 10%) was performed to determine the LVR. The sample gap was adjusted for each sample to obtain a normal force of 0.3 N. Mechanical spectra were recorded at a deformation of γ = 0.1% and a frequency between 0.01–100 Hz.[3] Exemplary curved for oscillatory rheology measurements are shown in the ESI† (Fig. S2). All measurements were carried out at 25 °C.

Gel yield and equilibrium degree of swelling. To determine the gel yield and equilibrium degree of swelling (EDS), the sample mass was determined directly after crosslinking (m_0). Afterward, the samples were swollen for 48 h in PBS. Furthermore, the dry weight of samples was determined by drying the swollen samples at 60 °C for three days. Both swelling and drying were performed until a constant sample weight was reached, which indicates that the equilibrium swollen state, or the complete removal of water was achieved. The gel yield was determined according to

$$Y = \frac{m_0}{m_d \cdot c_{GelMA}} \times 100\%, \quad (1)$$

with m_d being the dry mass. The EDS was determined according to

$$EDS = \frac{m_s}{m_d} \times 100\%, \quad (2)$$

with m_s being the mass of the swollen hydrogel.

2.6 Cell culture

Primary (HCK) and immortalized (HCKi) human corneal keratocytes were purchased from Innoprot. Cell culture medium (2% fetal bovine serum (FBS), 1% fibroblast growth supplement (FGS), 1% penicillin/streptomycin (P/S)) was purchased from Innoprot. HCK and HCKi were expanded in medium, according to the supplier's instructions and using standard culture conditions (37 °C, 5% CO_2). Cells were passaged when they reached 70–80% confluency using trypsin-EDTA at room temperature. For all experiments, cells from passages 8–15 (HCKi) or 2–3 (HCK) were used. HCK were cultured on collagen-coated dishes.

2.7 Toxicity tests

Formulation toxicity tests. The cytotoxicity of the hydrogel formulation was assessed by following a protocol proposed by Utama *et al.*[40] 1×10^6 cells g^{-1} HCKi were suspended in 30 wt% GelMA solutions containing 190 mmol L^{-1} riboflavin and various arginine hydrochloride concentrations. After incubating the cells for 1 h at room temperature, cell suspensions were diluted to 12 000 cells mL^{-1}, and the viability was determined *via* trypan blue staining using a Luna cell counter (logos biosystems, US). 200 μL were seeded into a 96-well plate and cultured for three days. Afterward, the medium was replaced by washing the cells three times with cell medium. The metabolic activity was determined using the MTT assay. Cells suspended in cell medium was used as a negative control and set to 100% metabolic activity. Cells treated with 60 μl of 1 wt% SDS were used as positive control.

Phototoxicity tests. The phototoxicity was assessed by suspending HCKi in different media (PBS, cell culture medium, or cell culture medium supplemented with 190 μmol L^{-1} riboflavin) at a density of 62 500 cells mL^{-1}. 40 μl of the cell suspension was pipetted in triplicates into a 96-well plate and immediately irradiated with blue light (455 nm LED, Thorlabs, Germany) using various intensities and irradiation times. Wells that were not irradiated were covered with an aluminum foil to keep samples in the dark. After irradiation, 60 μl of respective medium was added to each well and the cells were cultured for 3 days. Afterward, the metabolic activity was determined using the MTT assay. Non-irradiated cells were used as negative

control and set to 100% metabolic activity. Cells treated with 60 µl of 1 wt% SDS were used as positive control.

2.8 Cell encapsulation

Solutions for cell encapsulation contained 2.3 × 10^6 cells g^{-1}, 30 wt% GelMA, 190 µmol L^{-1} riboflavin and various concentrations of arginine hydrochloride. The hydrogel formulation was pipetted into a cylindrical mold with a diameter of 4 mm and a height of 2 mm. The samples were irradiated for different times with blue light (455 nm LED, Thorlabs, Germany) at an intensity of 4.3 mW cm^{-2}. After crosslinking, the samples were immediately placed in 1 mL cell culture medium and incubated for 1 h. Afterward, the cell culture medium was changed and the samples were incubated in 500 µL cell culture medium. For the encapsulation of HCKi, different arginine concentrations and irradiation times were used, whereas HCK were encapsulated using an arginine concentration of 80 mmol L^{-1} and an irradiation time of 10 min. The GelMA used for encapsulation with an irradiation time of 2 min had a DM of 0.85 mmol g^{-1}, whereas the GelMA used for all other samples had a DM of 0.77 mmol g^{-1}. The samples were cultured for 10 days. A medium change was performed every two days.

2.9 Cell analysis

Live/dead staining. After 1, 3, 7 and 10 days, live/dead staining was performed to assess the viability post encapsulation. To this end, the samples were washed with PBS for 1 h before they were stained with calcein-AM and ethidium homodimer (0.05% (v/v) and 0.2% (v/v) in 500 µL PBS, respectively) for 30 min. Samples treated with ethanol were used as positive control for cell death. For each sample, a section of ≈550 µm was imaged (step size 6.9 µm, 65 images). The total imaged sample volume was 0.65 mm^3. Viability of HCKis was determined by dividing the number of live cells by the total cell number.

Phalloidin and Hoechst staining. Samples were fixed on day 10 post-encapsulation. To this end, samples were immersed in 500 µL 4% paraformaldehyde for 20 min and cut in half. After washing the samples with PBS (3 times, 5 min), cells were permeabilized with Triton X-100 (0.1% (v/v) in PBS) for 30 min. Samples were stained with phalloidin – AF488 (2.5% (v/v) in 600 µL PBS, 2 h, RT). After washing 3 times with 20% donkey serum, samples were stained with 600 µL Hoechst in PBS (5 µg mL^{-1}, 20 min, RT). The samples were imaged with confocal fluorescence microscopy (LSM780, Zeiss, Germany). To ensure that cells inside the samples are visualized, samples were placed on the glass plate with the cut facing downwards. Imaris software (version 10.1.1) was used to render obtained images.

Immunostaining. Samples were fixed on day 10 post-encapsulation. To this end, samples were immersed in 500 µL 4% paraformaldehyde for 20 min and cut in half. Fixed samples were placed in 200 µL permeabilizing buffer (0.2% Triton X-100 in PBS) for 30 min. Afterward, the samples were placed in blocking buffer (5% goat serum, 5% donkey serum and 0.1% Triton X-100) for 2 h. The samples were washed three times for 10 min with PBS and placed in the primary antibody solution for 4 h (ALDH1-A1: 1:200; ALDH3-A1: 1:200, Lumican: 1:100, Keratocan: 1:100, respectively). Afterward, the samples were again washed in PBS three times for 10 min and stored in PBS at 8 °C until staining with secondary antibodies (goat against mouse AF488, 1:400 and donkey against rabbit AF647, 1:400 in PBS, 5 µg mL^{-1} Hoechst). The samples were incubated for 4 h and washed in PBS three times for 10 min. The samples were imaged with confocal fluorescence microscopy (LSM780, Zeiss, Germany). To ensure that cells inside the samples are visualized, samples were placed on the glass plate with the cut facing downwards. Imaris software (version 10.1.1) was used to render obtained images.

2.10 Statistical analysis

Statistical analysis was performed using two-way analysis of variance (ANOVA) with Tukey's *post hoc* test or Student's *t*-test, depending on the number of comparisons. Prism Graph Pad (Version 10.1.1) was used for statistical analysis. Oscillatory Rheology, Rotational Rheology, and Gel Characterization were performed using three individual samples and performing one measurement per sample. Formulation toxicity experiments were performed using three experiments per condition, and using three technical replicates per experiment for the metabolic assay. This resulted in a total of nine replicates per condition. Phototoxicity experiments were performed in one experiment per condition, using three technical replicates per experiment for the metabolic assay, resulting in a total of three replicates per condition. For encapsulation experiments, a minimum of 21 individual samples were produced during one experiment per condition, using three individual samples and one positive control for cell death for live/dead staining at a defined time point. A replicate set of samples was used for each time point. Thus, four samples were analyzed for each time point resulting in a total of 16 samples for each condition. Three individual samples were used for phalloidin/Hoechst staining and immunostaining, respectively. All imaging was performed on three individual samples, characterizing at least two different regions within one sample. All data are reported as average ± SD.

3. Results and discussion

3.1 Photocrosslinking behavior

The crosslinking behavior of RA-GelMA solutions was assessed *via* photorheology (Fig. 1(A)). When analyzing the gel point t_g, we found that both the GelMA concentration and the arginine concentration have a strong influence on the speed of network formation. When increasing the polymer concentration from 10 wt% to 30 wt% (Fig. 1(B)) at a constant riboflavin and arginine concentration, a reduction of the gel point t_g was noted from 300 s to 40 s. A similar trend was observed when varying the arginine concentration at a constant riboflavin and GelMA concentration (Fig. 1(C)). In this case, t_g decreased from 180 s (c_A = 0 mmol mL^{-1}) to 42 s (c_A = 610 mmol mL^{-1}). The decreased gel point for higher GelMA and arginine concentrations can be justified by either the increased amount of

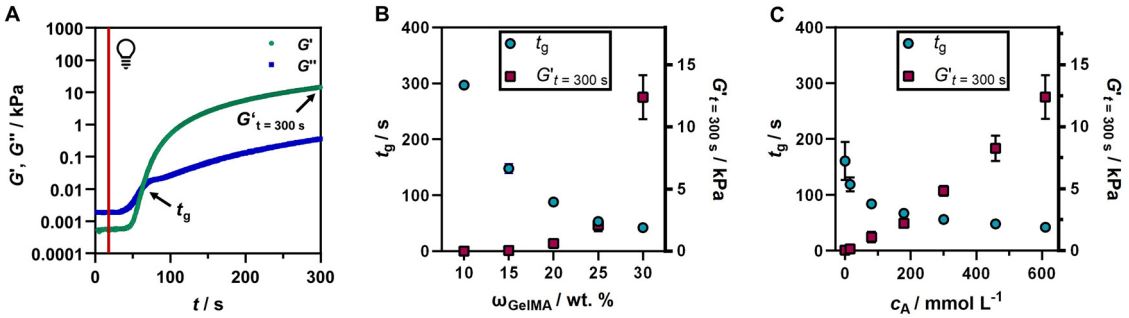

Fig. 1 (A) Storage (G') and loss (G'') moduli of RA-GelMA in different time points during an exemplary photorheology measurement (ω_{GelMA} = 30 wt%, c_A = 610 mmol L^{-1}). The analyzed parameters are marked in the figure. (B) Gelation time t_g and G' after 300 s for varying GelMA (c_A = 610 mmol L^{-1}). (C) Gelation time t_g and G' after 300 s for varying arginine concentrations (ω_{GelMA} = 30 wt%). The riboflavin concentration was 190 μmol L^{-1} in all samples.

polymerizable groups present in the GelMA polymer solution, or the increased number of radicals produced by the presence of arginine, for which both might speed up the network formation. Interestingly, t_g tails off at high GelMA and arginine concentrations, which means that network formation does not seem to be faster when increasing the polymer and co-initiator concentration at already high concentrations. However, when analyzing the storage modulus of the sample at the end of the measurement $\left(G'_{t=300\,s}\right)$, it can be seen that the storage modulus steadily increases even at high concentrations. The storage modulus at the end of crosslinking has important practical implications regarding the gel handling as samples with a low storage modulus tend to disintegrate after being produced. For different arginine and GelMA concentrations, storage moduli between 0.05–12.5 kPa were obtained. In addition, the delay time t_d, which quantifies the onset of crosslinking, as well as the crosslinking rate $\frac{\Delta G'}{\Delta t}$ were determined (Fig. S1, ESI†). Similar trends can be seen for these parameters. The delay time decreases with increasing GelMA or arginine concentrations and tails off at higher concentrations, while the crosslinking rate steadily increases. Comparing the data obtained in this study to photorheology data of GelMA being crosslinked by UV-A light using photoinitiators such as Irgacure or LAP, we observed that crosslinking of RA-GelMA is generally slower.[24,41] This might be due to the lower energy of blue light compared to UV-light, or even due to the different photoinitiation mechanism of the riboflavin/arginine system compared to Irgacure or LAP. We noted, however, that even though the crosslinking is slower compared to standard systems, t_g was reached for all examined concentrations. The obtained results also show that t_g and $G'_{t=300\,s}$ can be adjusted by varying the GelMA and arginine concentration.

3.2 Gel characterization

To examine the properties of RA-GelMA hydrogels, the storage modulus, gel yield, and equilibrium swelling degree were measured. A polymer content of 30 wt% was used to produce the hydrogels, as t_g was reached the fastest at this concentration and $G'_{t=300\,s}$ was highest. Fig. 2 depicts images of the uncrosslinked polymer solution (Fig. 2(A)), a sample directly after crosslinking (Fig. 2(B)), and a sample swollen to equilibrium (Fig. 2(C)). We observed that the polymer solution has a distinct yellow coloration caused by the riboflavin. After crosslinking and swelling, transparent hydrogels were obtained, and the yellow coloration could be washed out.

Next, we evaluated the storage modulus G', the gel yield Y and the equilibrium swelling degree EDS of RA-GelMA hydrogels prepared using different co-initiator concentrations, irradiation times and irradiation intensities (Fig. 2(D)). G' cannot be directly compared to the storage moduli obtained by photorheology measurements in Section 3.1, as those samples have not been swollen to equilibrium. We found that the storage moduli of prepared samples varied between 2.5 kPa and 17 kPa. These values are within the typical range of G' obtained for GelMA-based hydrogels,[3,42,43] although it should be mentioned that comparable values are obtained for lower GelMA concentrations. This might be due to using a lower-energy blue light source, and the different photoinitiation mechanism of the riboflavin/arginine system, resulting in less effective crosslinking. All tested parameters have an influence on G' and correlated positively with it, which demonstrates that the storage modulus of RA-GelMA hydrogels crosslinked by blue light can be adjusted by varying the co-initiator concentration, irradiation intensity or irradiation time. This is particularly important for potential applications in tissue engineering, as native tissues have a wide range of dynamic properties[44] and cells are highly influenced by the hydrogel's viscoelastic properties.[45] For human corneal tissue specifically, Young's moduli between E = 7.5–110 kPa have been measured for different layers (7.5 ± 4.2 kPa – anterior basement membrane, 109.8 ± 13.2 kPa – Bowman's layer, 33.1 ± 6.1 kPa – anterior stroma, 50 ± 17.8 kPa – Descemet's membrane, all measured *via* atomic force microscopy).[46] For elastic materials, the relation between E and G' is given as[47]

$$E = 2G'(1 + \nu), \quad (3)$$

where ν represents the Poisson's ratio (ν = 0.4 for corneal tissue[48]). According to eqn (3), calculated storage moduli for human corneal tissue are G'_{calc} = 2.7 ± 1.5 kPa – anterior basement membrane, 39 ± 4.7 kPa – Bowman's layer, 11.8 ± 2.2 kPa – anterior stroma, and 17.9 ± 6.4 kPa – Descemet's membrane, leaving the values of hydrogels investigated in this study in the

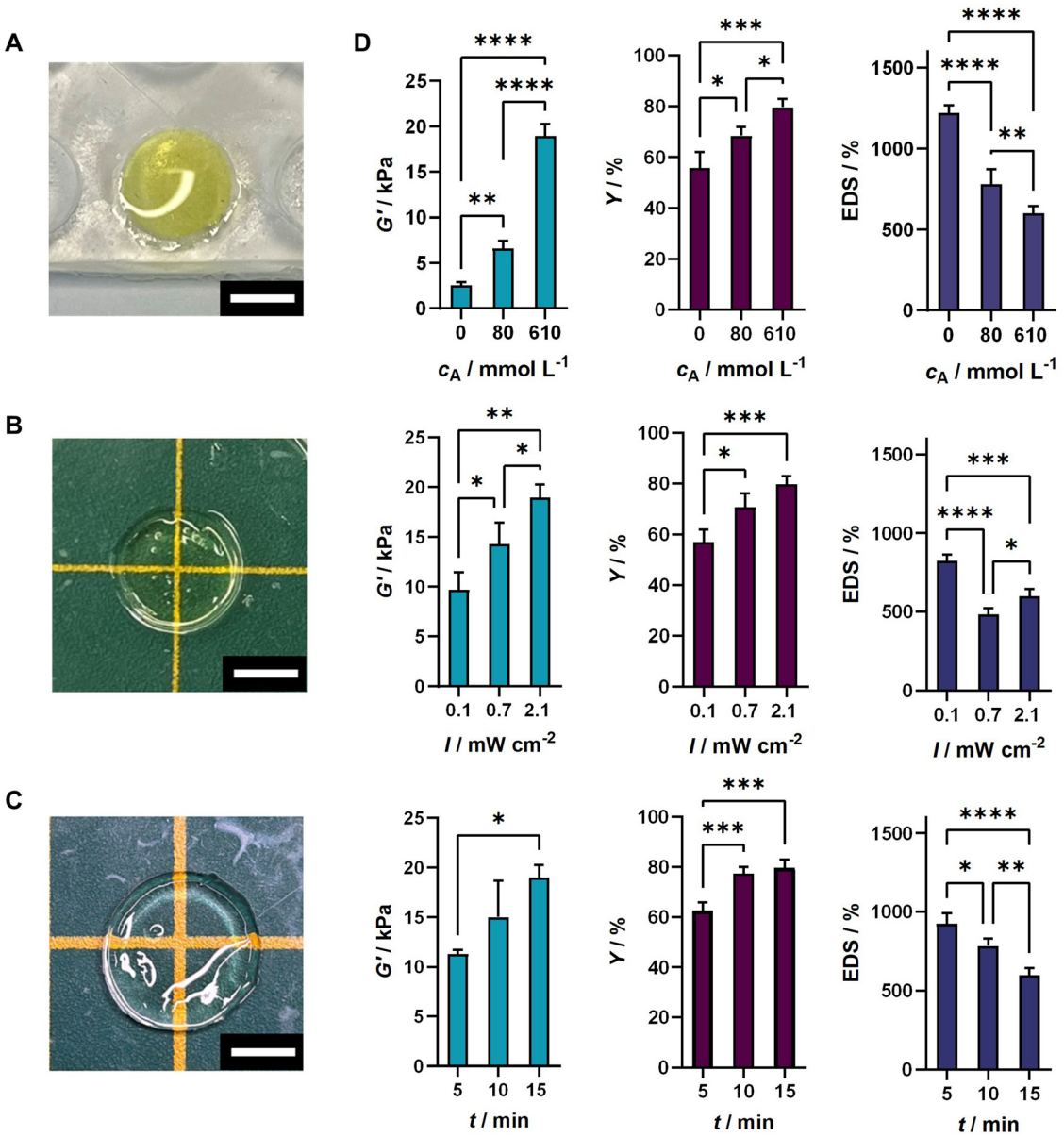

Fig. 2 (A) Images of uncrosslinked RA-GelMA formulation pipetted into a PDMS mold, (B) sample directly after crosslinking and (C) sample swollen to equilibrium (ω_{GelMA} = 30 wt%, c_A = 0 mmol mL^{-1}, c_{Ribo} = 190 μmol L^{-1}). The scale bars are 500 μm. (D) Effect of arginine concentration, irradiation time and irradiation intensity on the storage modulus (f = 1 Hz, γ = 0.1%), the gel yield and the equilibrium swelling degree of RA-GelMA hydrogels (ω_{GelMA} = 30 wt%, c_{Ribo} = 190 μmol L^{-1}). If not denoted otherwise, the arginine concentration is 610 mmol L^{-1}, the irradiation intensity is 2.1 mW cm^{-2} and the irradiation time is 15 min. P-Values: *$p < 0.05$, **$p < 0.01$, ***$p < 0.001$, ****$p < 0.0001$.

range of calculated values for the anterior basement membrane and the anterior stroma.

The gel yield, which is related to the efficiency of crosslinking, is between 56% to 80%. All tested parameters correlate positively with the gel yield. Thus, crosslinking is most efficient when using high levels of co-initiator concentrations, irradiation times and irradiation intensities. GelMA-based hydrogels crosslinked with Irgacure 2959 and UV light typically have gel yields in the range of 90–100%, depending on the polymer concentration.[3] In this study, we show that RA-GelMA hydrogels behave differently compared to standard systems, having less efficient crosslinking.

RA-GelMA gels showed equilibrium degree of swelling (EDS) values between 480 and 1200%. The tested parameters were inversely correlated with the EDS, which demonstrates that the EDS can also be adjusted by varying the co-initiator concentration, irradiation time or irradiation intensity. The results are similar to the typical range of EDS values for other photocrosslinked GelMA-based hydrogels, although those data were obtained for lower polymer concentrations.[3,7,49] The use of a higher polymer content is typically associated with a higher viscosity and is therefore often avoided. However, the viscosity of a 30 wt% RA-GelMA formulation is between 60–45 mPa s (Fig. S3, ESI†), which is due to the high methacryloylation

degree of GelMA and allows for easy pipetting, even at a high polymer content.

Hydrogels examined in this study were exposed to oxygen during crosslinking, which is usually avoided by covering the polymer solution with a glass pane.[9,50] However, no negative effects, such as irregular swelling or incomplete crosslinking due to oxygen inhibition were observed, and samples still had a flat surface required for oscillatory rheology. In fact, when comparing samples crosslinked with reduced oxygen exposure (*i.e.* covered with a glass pane during crosslinking) to samples crosslinked in presence of oxygen, slightly higher values for G' were observed for the latter (Fig. S4, ESI†). This effect seems to be more pronounced under unfavorable crosslinking conditions, (*e.g.* low co-initiator concentrations, irradiation times or intensities) and can be ascribed to the formation of singlet oxygen in riboflavin-mediated crosslinking, [17] which might have a supporting effect on the network formation. This is in stark contrast to commonly used type I photoinitiators, where oxygen has a negative effect on the crosslinking process.[51] Precise quantification and analysis of this effect is subject of further studies. Looking at the EDS and gel yield, no clear trend could be seen.

3.3 Toxicity tests

To assess whether the formulation and crosslinking conditions are biocompatible, cytotoxicity tests were carried out using immortalized human corneal keratocytes (HCKi). Firstly, cells were exposed to various hydrogel formulations with different arginine concentrations, assessing the viability after 1 h exposure (Fig. 3(A)). In addition, we determined the metabolic

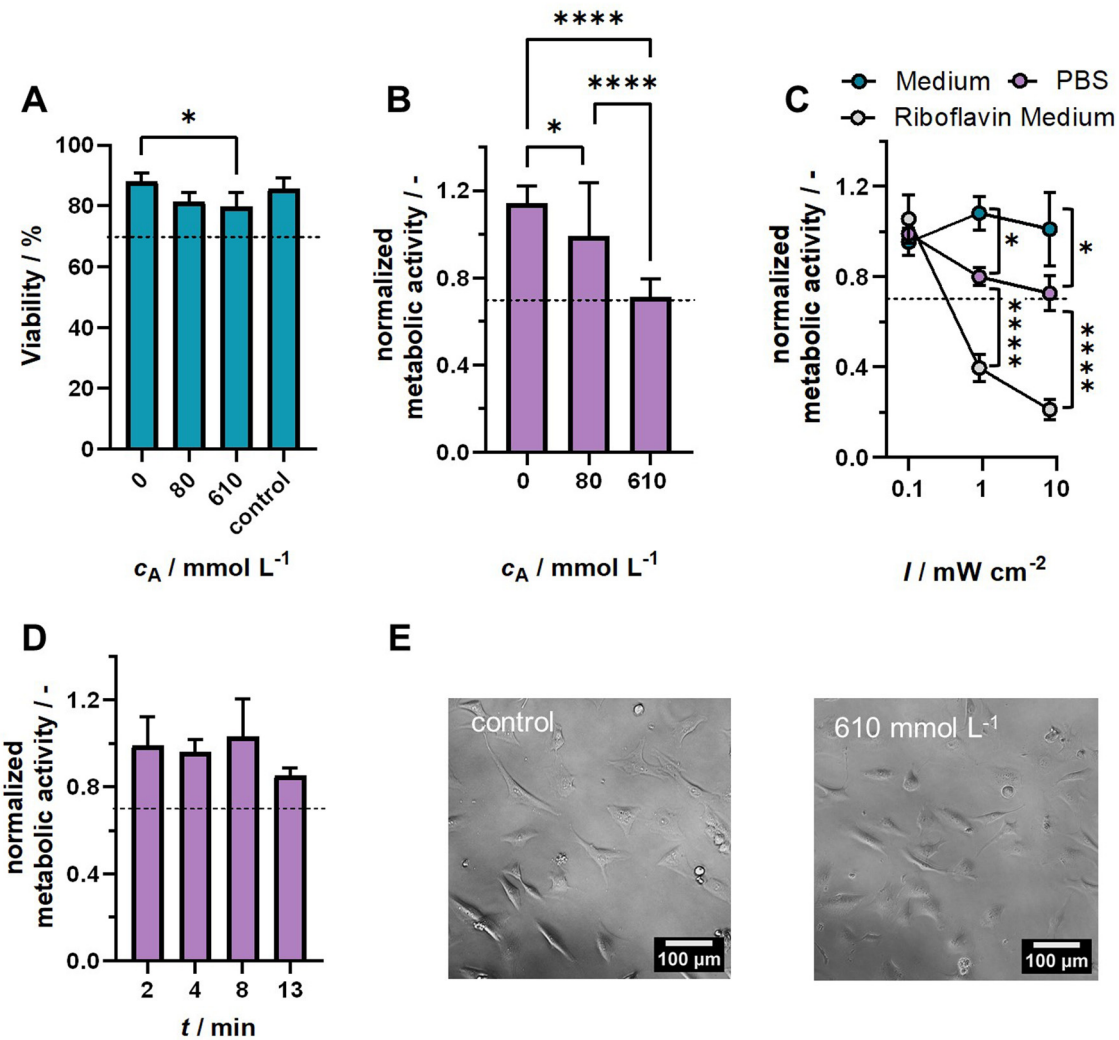

Fig. 3 (A) Viability determined *via* trypan blue staining after 1 h exposure of HCKi to hydrogel formulation (ω_{GelMA} = 30 wt%, c_{Ribo} = 190 µmol L^{-1}) with different arginine concentrations. (B) Normalized metabolic activity determined *via* the MTT assay on day 3 of culture after exposure to hydrogel formulations. (C) Normalized metabolic activity determined *via* the MTT assay on day 3 of culture after exposure to blue light (t = 2 min) at different intensities. (D) Normalized metabolic activity determined *via* the MTT assay on day 3 of culture after exposure to blue light (I = 10 mW cm^{-2}) for different irradiation times. (E) Images of cells on day 3 of culture after exposure to cell medium (control) or hydrogel formulation containing 610 mmol L^{-1} arginine. The scale bar is 100 µm. *P*-Values: *$p < 0.05$, **$p < 0.01$, ***$p < 0.001$, ****$p < 0.0001$. The dashed line marks 70% viability or 0.7 normalized metabolic activity.

activity after reseeding, and after three days of culture (Fig. 3(B)). HCKi viability determined after 1 h exposure slightly decreased with increasing arginine concentration, but stayed over 70% even at the highest co-initiator concentration. A viability of 70% is considered the threshold for cytotoxic potential.[52] Notably, the viability for different hydrogel formulations did not differ significantly from the control sample (cells suspended in medium). Assessing the metabolic activity after reseeding, and after three days of culture, we observed that the metabolic activity significantly decreased with increasing co-initiator concentration of 70%

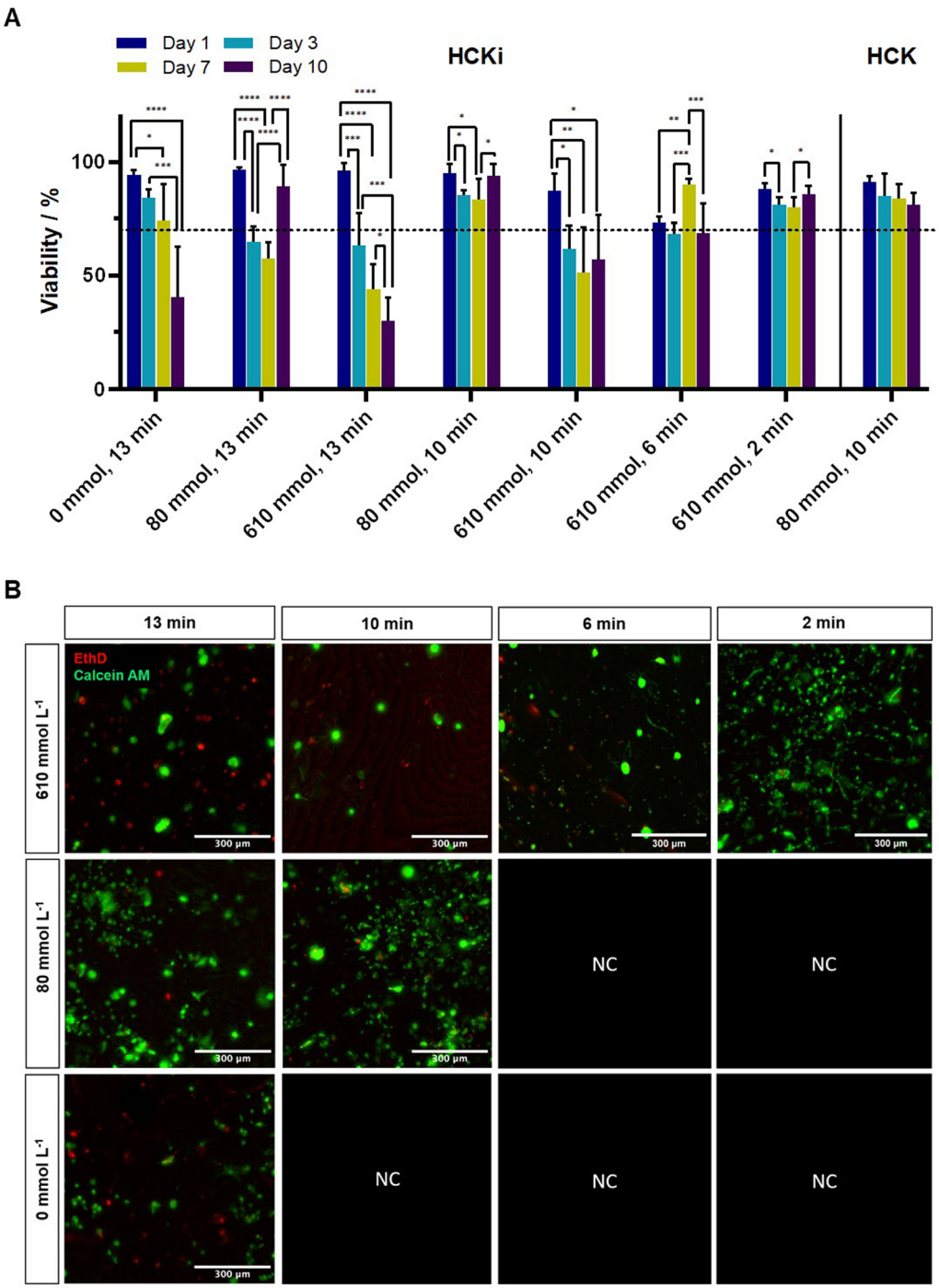

Fig. 4 (A) Influence of arginine concentration and irradiation time on the viability of encapsulated human corneal keratocytes on different days post-encapsulation (ω_{GelMA} = 30 wt%, c_{Ribo} = 190 µmol L^{-1}). The dashed line marks 70% viability. (B) Images obtained by live/dead staining of encapsulated HCKi on day 10 for different arginine concentrations and irradiation times. Samples marked with NC could not be fully crosslinked and were therefore not analyzed. The DM of used GelMA was 0.77 mmol g^{-1}, except for samples crosslinked with an irradiation time of 2 min, for which GelMA with a DM of 0.85 mmol g^{-1} was used. The irradiation intensity was 4.3 mW cm^{-2}. *P*-Values: *$p < 0.05$, **$p < 0.01$, ***$p < 0.001$, ****$p < 0.0001$. The dashed line marks 70% viability. The scale bar is 300 µm.

for c_A = 610 mmol mL^{-1}. Nonetheless, this value is at the threshold for cytotoxic potential, and cell morphology did not differ from non-treated cells. These results show that higher co-initiator concentrations have an effect on cell behavior, which should be considered when using RA-GelMA for keratocyte encapsulation.

Next, we assessed the effect of blue light irradiation on cells suspended in different media (Fig. 3(C)). Cells suspended in PBS showed a decrease in metabolic activity with increasing irradiation intensity. By contrast, this effect was not observed when suspending cells in cell culture medium, even for prolonged irradiation times (Fig. 3(D)). This difference might be justified by the absorption of blue light by phenol red, which is a component of the cell culture medium, or the presence of nutrients in cell culture medium. When adding 190 µmol L^{-1} riboflavin to the cell culture medium (c_A = 0 mmol L^{-1}), the metabolic activity strongly decreased with increasing light

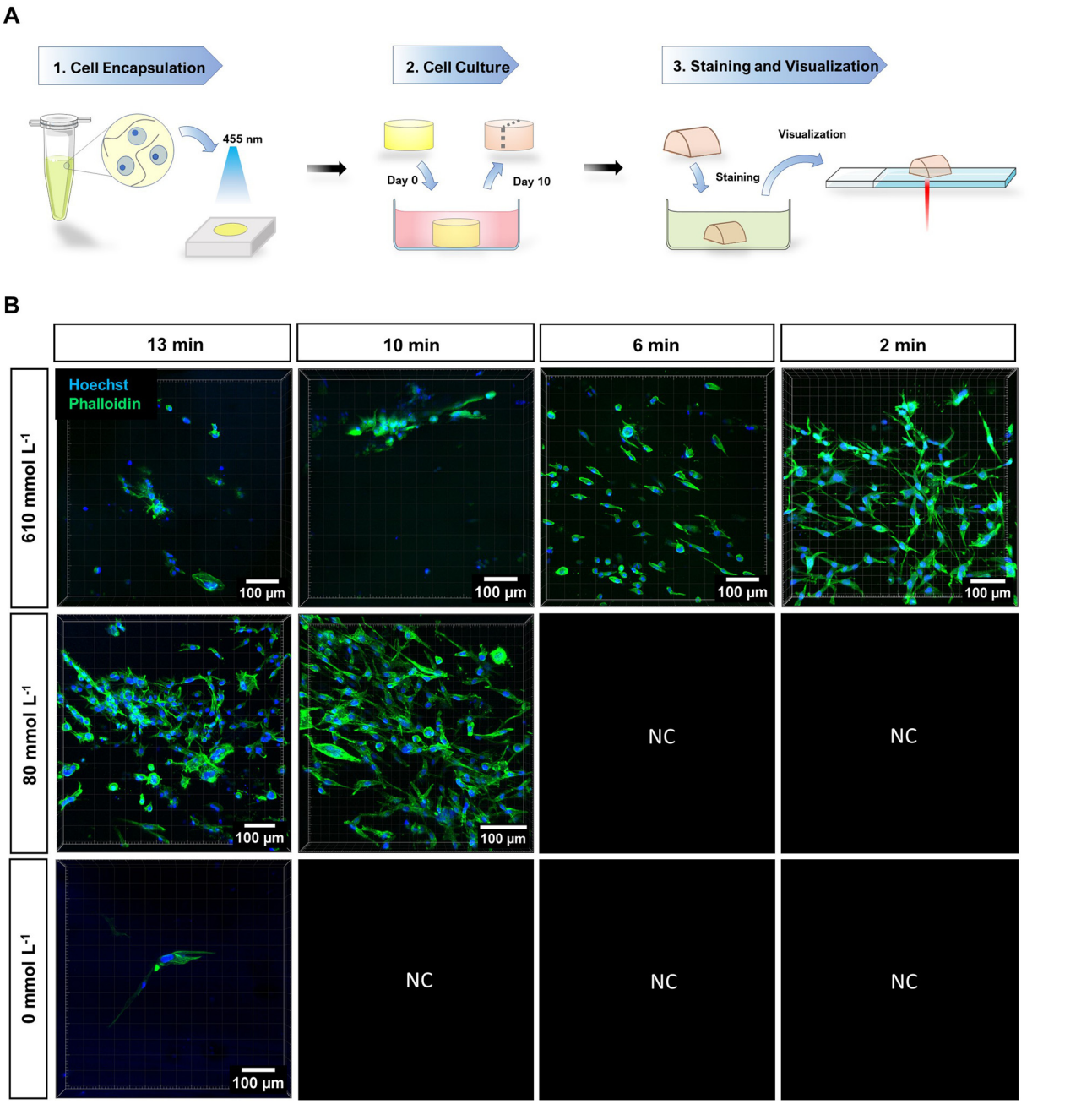

Fig. 5 (A) Procedure of cell encapsulation and visualization for confocal fluorescence microscopy. The figure was created using bioicons.com. (B) Rendered images of phalloidin/Hoechst stained HCKi on day 10 post encapsulation (ω_{GelMA} = 30 wt%, c_{Ribo} = 190 µmol L^{-1}) for different arginine concentrations and irradiation times. Samples marked with NC could not be fully crosslinked and were therefore not analyzed. The DM of used GelMA was 0.77 mmol g^{-1}, except for samples crosslinked with an irradiation time of 2 min, for which GelMA with a DM of 0.85 mmol g^{-1} was used. The irradiation intensity was 4.3 mW cm^{-2}. The scale bar is 100 µm.

intensity. This is due to the formation of radicals that can harm cells, which has also been previously documented in studies using synthetic photoinitiators like LAP.[8] During cell encapsulation, however, radicals are also caught by the reactive groups on polymer chains.

3.4 Cell encapsulation

To examine the potential application of RA-GelMA in corneal tissue engineering, both immortalized (HCKi) and primary (HCK) human corneal keratocytes were encapsulated inside the hydrogel (ω_{GelMA} = 30 wt%, c_{Ribo} = 190 μmol L^{-1}). Conditions for cell encapsulation were first optimized for immortalized cells by examining cell viability at different time points post-encapsulation, when using different irradiation times and co-initiator concentrations. This was done to provide a large number of samples, as HCKi grow faster compared to HCK. The optimum condition was then chosen for encapsulation of primary cells. For encapsulation experiments, cell culture medium was used to prepare the RA-GelMA solution, since no effect of blue light on the metabolic activity was observed during the phototoxicity tests (Section 3.3).

HCKi encapsulation. The viability of encapsulated HCKi was examined for three different co-initiator concentrations (0, 80 and 610 mmol L^{-1}), and four different irradiation times (13, 10, 6 and 2 min). To minimize the exposure of cells to blue light and radicals, the least amount of time needed to obtain a fully crosslinked gel for each co-initiator concentration (13 min for c_A = 0 mmol L^{-1}, 10 min for c_A = 80 mmol L^{-1}, 6 min for c_A = 610 mmol L^{-1}) was chosen as irradiation time. For c_A = 610 mmol L^{-1}, cell encapsulation was also tested using GelMA with a slightly higher DM (0.85 mmol g^{-1} instead of 0.77 mmol g^{-1}), with which the irradiation time could be reduced to 2 min. The viability of encapsulated cells was determined *via* live/dead staining at different time points post-encapsulation (Fig. 4(A)). Images of cells stained 10 days post-encapsulation are shown in Fig. 4(B). We observed increased cell viability with decreasing irradiation time and decreasing co-initiator concentration. This is observed given that there are less cytotoxic radicals at lower irradiation times. Similar trends have been seen in cells encapsulated in GelMA-based hydrogels by UVA-initiated crosslinking.[53] HCKi morphology stained with phalloidin and Hoechst was visualized *via* confocal fluorescence microscopy. Fig. 5(A) depicts a scheme for cell encapsulation as well as subsequent staining and visualization. Confocal fluorescence microscopy images of stained cells are depicted in Fig. 5(B). Cell spreading was more often observed in hydrogels exposed to less irradiation time and lower co-initiator concentration. Images of masked cells and nuclei are depicted in the ESI† (Fig. S5). We identified two RA-GelMA formulations that maintained a high cell viability over the course of 10 days, and allowed for the longest cell filopodia elongations: (1) c_A = 80 mmol L^{-1} and 10 min irradiation time, and (2) c_A = 610 mmol L^{-1} and 2 min irradiation time.

HCK encapsulation. HCK were encapsulated using an irradiation time of 10 min and a co-initiator concentration of 80 mmol L^{-1} (ω_{GelMA} = 30 wt%, c_{Ribo} = 190 μmol L^{-1}). A co-initiator concentration of 610 mmol L^{-1} was not used for encapsulation,

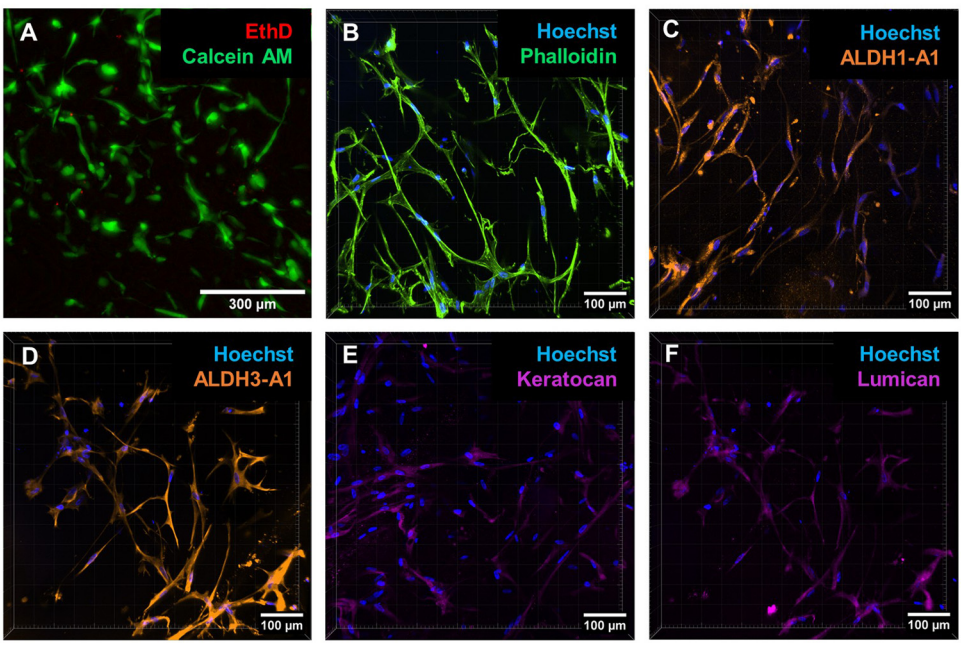

Fig. 6 (A) Images obtained by live/dead staining of encapsulated HCK. The scale bar is 300 μm. (B) Rendered images obtained by Phalloidin staining of encapsulated HCK. (C) Immunostaining of encapsulated HCK for ALDH1-A1. (D) Immunostaining of encapsulated HCK for ALDH3-A1. (E) Immunostaining of encapsulated HCK for Keratocan. (F) Immunostaining of encapsulated HCK for Lumican. Hoechst was added to images (B)–(F) to visualize the nucleus. The scale bar in Fig. 6 (B)–(F) is 100 μm. All images were taken 10 days post encapsulation (ω_{GelMA} = 30 wt%, c_{Ribo} = 190 μmol L^{-1}, c_A = 80 mmol L^{-1}, t = 10 min, I = 4.3 mW cm^{-2}).

as cells showed a decreased metabolic activity in cytotoxicity tests (Fig. 3(B)). By contrast, a prolonged irradiation time yielded no significant effect on the metabolic activity (Fig. 3(D)). Encapsulated HCK showed high viability (>80%) over the course of 10 days (Fig. 4(A) and 6(A)), and pronounced cell spreading on day 10 (Fig. 6(B)). A masked image is depicted in the ESI† (Fig. S6). Qualitative analysis of immunostaining images revealed that characteristic stromal corneal keratocyte markers (ALDH1-A1, ALDH3-A1, Keratocan and Lumican) were positively expressed (Fig. 6(C)–(F)). This demonstrates that the HCK phenotype is conserved *in vitro* up to 10 days after encapsulation. The encapsulation of HCK in GelMA-based hydrogels has been examined in very few previous studies, using Irgacure 2959 and UV-A light for crosslinking.[54,55] In these studies, similar cell spreading was observed, although data for cell viability is only shown up to day 2.[55] Other parameters such as the expression of typical keratocyte markers or the viability past day 3 after encapsulation were not assessed.[54,55] Cells encapsulated in RA-GelMA show comparable properties to cells encapsulated in collagen-based materials,[56] which are the gold-standard used in corneal tissue engineering due to the high collagen content of corneal stroma. However, handling of collagen gels is often challenging due to the long polymerization times, and the low solubility of collagen at neutral pH. In contrast, RA-GelMA shows much better processability and easier handling.

4. Conclusion

In this study, we synthesized and characterized for the first time RA-GelMA hydrogels using riboflavin and arginine as a biobased photoinitiation system. We showed that crosslinking can be initiated with blue light, and that the gelation point can be controlled by adjusting the GelMA content, or the arginine concentration. Furthermore, we provided a thorough characterization of the produced materials. Cytotoxicity tests showed that RA-GelMA and external crosslinking conditions are non-cytotoxic. Human corneal keratocytes encapsulated in RA-GelMA showed a high degree of cell spreading as well as native keratocyte phenotype maintenance, thus demonstrating that the new formulation is a promising candidate for corneal tissue engineering. Due to its low viscosity and adjustable properties, the RA-GelMA formulation also shows high promise for corneal bioprinting studies. The developed RA-GelMA formulation can provide an alternative to existing crosslinking strategies by using a sustainable and cell friendly photoinitiation system which offers the possibility of visible light induced crosslinking.

Author contributions

Friederike Dehli: conceptualization, investigation, supervision, writing – original draft. Olivia Schless: investigation. Meret Kaliske: investigation. Isabel Potthof: investigation. Alexandre Taoum: writing – review and editing. Matthias Fuest: writing – review and editing. Daniela Duarte Campos: conceptualization, writing – review and editing.

Data availability

The data supporting this article have been included as part of the ESI.†

Conflicts of interest

The authors declare no conflict of interest.

Acknowledgements

This work was supported by the Bundesministerium für Bildung und Forschung (BMBF, grant number 13XP5135 to DDC). This work was supported by the Deutsche Forschungsgemeinschaft (DFG, German Research Foundation) under Germany's Excellence Strategy *via* the Excellence Cluster 3D Matter Made to Order (EXC-2082/1-390761711 to DDC). FD gratefully acknowledges funding from the Cluster of Excellence 3D Matter Made to Order (3DMM2O, PostDoc take-off grant 2024). The authors thank the Biomechanics Core Facility at the Institute for Molecular Systems Engineering and Advanced Materials (IMSEAM). The authors thank Prof. Dr Gert Fricker for the use of their titrator, and Prof. Dr Franziska Thomas and Dr Bernhard Wetterauer for the use of their freeze-dryers.

References

1 J. W. Nichol, S. T. Koshy, H. Bae, C. M. Hwang, S. Yamanlar and A. Khademhosseini, *Biomaterials*, 2010, **31**, 5536–5544.
2 B. J. Klotz, D. Gawlitta, A. J. W. P. Rosenberg, J. Malda and F. P. W. Melchels, *Trends Biotechnol.*, 2016, **34**, 394–407.
3 E. Hoch, C. Schuh, T. Hirth, G. E. M. Tovar and K. Borchers, *J. Mater. Sci.: Mater. Med.*, 2012, **23**, 2607–2617.
4 T. C. Lai, J. Yu and W. B. Tsai, *J. Mater. Chem. B*, 2016, **4**, 2304–2313.
5 A. H. Nguyen, J. McKinney, T. Miller, T. Bongiorno and T. C. McDevitt, *Acta Biomater.*, 2015, **13**, 101–110.
6 J. Yin, M. Yan, Y. Wang, J. Fu and H. Suo, *ACS Appl. Mater. Interfaces*, 2018, **10**, 6849–6857.
7 E. Hoch, T. Hirth, G. E. M. Tovar and K. Borchers, *J. Mater. Chem. B*, 2013, **1**, 5675–5685.
8 S. Stier, L. Rebers, V. Schönhaar, E. Hoch and K. Borchers, *J. Mater. Sci.: Mater. Med.*, 2019, **30**, 35.
9 E. Hoch, G. E. M. Tovar and K. Borchers, *Bioinspired, Biomimetic Nanobiomater.*, 2016, **5**, 51–66.
10 J. R. Choi, K. W. Yong, J. Y. Choi and A. C. Cowie, *Biotechniques*, 2019, **66**, 40–53.
11 J. P. Whitcher, M. Srinivasan and M. P. Upadhyay, *Bull. W. H. O.*, 2001, **79**, 214–221.
12 P. Gain, R. Jullienne, Z. He, M. Aldossary, S. Acquart, F. Cognasse and G. Thuret, *JAMA Ophthalmol.*, 2016, **134**, 167–173.

13 M. Zhang, F. Yang, D. Han, S. Yao Zhang, Y. Dong, X. Li, L. Ling, Z. Deng, X. Cao, J. Tian, Q. Ye and Y. Wang, *Int. J. Bioprint.*, 2023, **9**, 474–492.
14 L. J. Luo, J. Y. Lai, S. F. Chou, Y. J. Hsueh and D. H. K. Ma, *Acta Biomater.*, 2018, **65**, 123–136.
15 A. Isaacson, S. Swioklo and C. J. Connon, *Exp. Eye Res.*, 2018, **173**, 188–193.
16 C. Kilic Bektas and V. Hasirci, *Biomater. Sci.*, 2020, **8**, 438–449.
17 L. Fan, O. Jung, M. Herrmann, M. Shirokikh, S. Stojanovic, S. Najman, F. Körte, X. Xiong, K. Schenke-Layland and M. Barbeck, *Adv. Funct. Mater.*, 2024, **34**, 2401742.
18 A. I. Van Den Bulcke, B. Bogdanov, N. De Rooze, E. H. Schacht, M. Cornelissen and H. Berghmans, *Biomacromolecules*, 2000, **1**, 31–38.
19 Z. Dong, Q. Yuan, K. Huang, W. Xu, G. Liu and Z. Gu, *RSC Adv.*, 2019, **9**, 17737–17744.
20 B. Huber, K. Borchers, G. E. M. Tovar and P. J. Kluger, *J. Biomater. Appl.*, 2016, **30**, 699–710.
21 V. H. M. Mouser, F. P. W. Melchels, J. Visser, W. J. A. Dhert, D. Gawlitta and J. Malda, *Biofabrication*, 2016, **8**, 035003.
22 B. D. Fairbanks, M. P. Schwartz, C. N. Bowman and K. S. Anseth, *Biomaterials*, 2009, **30**, 6702–6707.
23 F. Dehli, L. Rebers, C. Stubenrauch and A. Southan, *Biomacromolecules*, 2019, **20**, 2666–2674.
24 C. D. O'Connell, B. Zhang, C. Onofrillo, S. Duchi, R. Blanchard, A. Quigley, J. Bourke, S. Gambhir, R. Kapsa, C. Di Bella, P. Choong and G. G. Wallace, *Soft Matter*, 2018, **14**, 2142–2151.
25 S. Pahoff, C. Meinert, O. Bas, L. Nguyen, T. J. Klein and D. W. Hutmacher, *J. Mater. Chem. B*, 2019, **7**, 1761–1772.
26 A. Al Mousawi, P. Garra, M. Schmitt, J. Toufaily, T. Hamieh, B. Graff, J. P. Fouassier, F. Dumur and J. Lalevée, *Macromolecules*, 2018, **51**, 4633–4641.
27 L. Breloy, V. Brezová, Z. Barbieriková, Y. Ito, J. Akimoto, A. Chiappone, S. Abbad-Andaloussi, J. P. Malval and D. L. Versace, *ACS Appl. Polym. Mater.*, 2022, **4**, 210–228.
28 H. Chen, G. Noirbent, K. Sun, D. Brunel, D. Gigmes, F. Morlet-Savary, Y. Zhang, S. Liu, P. Xiao, F. Dumur and J. Lalevée, *Polym. Chem.*, 2020, **11**, 4647–4659.
29 M. Rahal, H. Mokbel, B. Graff, J. Toufaily, T. Hamieh, F. Dumur and J. Lalevée, *Catalysts*, 2020, **10**, 1–18.
30 F. Raiskup-Wolf, A. Hoyer, E. Spoerl and L. E. Pillunat, *J. Cataract Refractive Surg.*, 2008, **34**, 796–801.
31 A. K. Nguyen, S. D. Gittard, A. Koroleva, S. Schlie, A. Gaidukeviciute, B. N. Chichkov and R. J. Narayan, *Regener. Med.*, 2013, **8**, 725–738.
32 I. Zaborniak, P. Chmielarz and K. Matyjaszewski, *Macromol. Chem. Phys.*, 2020, **221**, 1900496.
33 I. Zaborniak and P. Chmielarz, *Eur. Polym. J.*, 2021, **142**, 110152.
34 D. R. Cardoso, S. H. Libardi and L. H. Skibsted, *Food Funct.*, 2012, **3**, 487–502.
35 W. Pan, T. J. Wallin, J. Odent, M. C. Yip, B. Mosadegh, R. F. Shepherd and E. P. Giannelis, *J. Mater. Chem. B*, 2019, **7**, 2855–2864.
36 Y. C. Chen, T. Y. Liu and Y. H. Li, *J. Coat. Technol. Res.*, 2021, **18**, 99–106.
37 S. Sharifi, H. Sharifi, A. Akbari and J. Chodosh, *Sci. Rep.*, 2021, **11**, 23276.
38 C. Claaßen, M. H. Claaßen, V. Truffault, L. Sewald, G. E. M. Tovar, K. Borchers and A. Southan, *Biomacromolecules*, 2018, **19**, 42–52.
39 H. H. Winter and F. Chambon, *J. Rheol.*, 1986, **30**, 367–382.
40 R. H. Utama, V. T. G. Tan, K. C. Tjandra, A. Sexton, D. H. T. Nguyen, A. P. O'Mahony, E. Y. Du, P. Tian, J. C. C. Ribeiro, M. Kavallaris and J. J. Gooding, *Macromol. Biosci.*, 2021, **21**, 2100125.
41 A. K. Nguyen, P. L. Goering, R. K. Elespuru, S. S. Das and R. J. Narayan, *Polymers*, 2020, **12**, 1489.
42 V. Vassallo, A. Tsianaka, N. Alessio, J. Grübel, M. Cammarota, G. E. M. Tovar, A. Southan and C. Schiraldi, *J. Biomed. Mater. Res., Part A*, 2022, **110**, 1210–1223.
43 L. Sewald, C. Claaßen, T. Götz, M. H. Claaßen, V. Truffault, G. E. M. Tovar, A. Southan and K. Borchers, *Macromol. Biosci.*, 2018, **18**, 1800168.
44 C. Liu, Q. Yu, Z. Yuan, Q. Guo, X. Liao, F. Han, T. Feng, G. Liu, R. Zhao, Z. Zhu, H. Mao, C. Zhu and B. Li, *Bioact. Mater.*, 2023, **25**, 445–459.
45 O. Chaudhuri, J. Cooper-White, P. A. Janmey, D. J. Mooney and V. B. Shenoy, *Nature*, 2020, **584**, 535–546.
46 J. A. Last, S. M. Thomasy, C. R. Croasdale, P. Russell and C. J. Murphy, *Micron*, 2012, **43**, 1293–1298.
47 A. Kazaili, B. Geraghty and R. Akhtar, *J. Mech. Behav. Biomed. Mater.*, 2019, **100**, 103375.
48 E. Uchio, S. Ohno, J. Kudoh, K. Aoki and T. Kisielewicz, *Br. J. Ophthalmol.*, 1999, **83**, 1106–1111.
49 S. Chen, Y. Wang, J. Lai, S. Tan and M. Wang, *Biomacromolecules*, 2023, **24**, 2928–2941.
50 L. Rebers, T. Granse, G. Tovar, A. Southan and K. Borchers, *Gels*, 2019, **5**, 4.
51 S. C. Ligon, B. Husár, H. Wutzel, R. Holman and R. Liska, *Chem. Rev.*, 2014, **114**, 577–589.
52 **https://www.iso.org/standard/36406.html** for "Biological Evaluation of Medical Devices (ISO Standard No. 10993:2009).
53 H. Stratesteffen, M. Köpf, F. Kreimendahl, A. Blaeser, S. Jockenhoevel and H. Fischer, *Biofabrication*, 2017, **9**, 045002.
54 C. Kilic Bektas and V. Hasirci, *J. Mater. Sci.: Mater. Med.*, 2020, **31**, 2.
55 C. Kilic Bektas and V. Hasirci, *J. Tissue Eng. Regener. Med.*, 2018, **12**, e1899–e1910.
56 D. F. Duarte Campos, M. Rohde, M. Ross, P. Anvari, A. Blaeser, M. Vogt, C. Panfil, G. H. F. Yam, J. S. Mehta, H. Fischer, P. Walter and M. Fuest, *J. Biomed. Mater. Res., Part A*, 2019, **107**, 1945–1953.